Structure 14, 1369–1376, September 2006 ©2006 Elsevier Ltd All rights reserved DOI 10.1016/j.str.2006.06.016

Amyloid Formation May Involve α- to β Sheet Interconversion via Peptide Plane Flipping

E. James Milner-White,[1,*] James D. Watson,[3] Guoying Qi,[2] and Steven Hayward[2]
[1] Institute of Biomedical and Life Sciences
University of Glasgow
Glasgow, G12 8QQ
United Kingdom
[2] School of Computing Sciences and
School of Biological Sciences
University of East Anglia
Norwich, NR4 7TJ
United Kingdom
[3] EMBL-European Bioinformatics Institute
Wellcome Trust Genome Campus
Hinxton
Cambridge, CB10 1SD
United Kingdom

Summary

The toxic component of amyloid is not the mature fiber but a soluble prefibrillar intermediate. It has been proposed, from molecular dynamics simulations, that the precursor is composed of α sheet, which converts into the β sheet of mature amyloid via peptide plane flipping. α sheet, not seen in proteins, occurs as isolated stretches of polypeptide. We show that the α- to β sheet transition can occur by the flipping of alternate peptide planes. The flip can be described as $\alpha_R\alpha_L \leftrightarrow \beta\beta$. A search conducted within sets of closely related protein crystal structures revealed that these flips are common, occurring in 8.5% of protein families. The average "α_L" conformation found is in an adjacent and less populated region of the Ramachandran plot, as expected if the flanking peptide planes, being hydrogen bonded, are restricted in their movements. This work provides evidence for flips allowing direct α- to β sheet interconversion.

Introduction

α Sheet

In α helix and β sheet, the main chain conformations of successive residues are approximately the same. Alternatively the main chain conformations of successive residues are enantiomeric. Pauling and Corey (1951a, 1951b) suggested the existence of what is now called α sheet, illustrated in Figures 1A and 1I, in which successive residues alternate between α_R and α_L conformations. These are defined by the main chain dihedral angles ϕ and ψ: for α_R, $\phi = -60^\circ$ and $\psi = -60^\circ$; for α_L, $\phi = 60^\circ$ and $\psi = 60^\circ$ (the angles are shown in Figure 2B). To allow a view of its characteristic S-shaped, or wiggly, structure, the same polypeptide is shown in Figure 1D after rotation. The first structures of native proteins did not reveal any polypeptide like this, and for a few decades, the idea was largely forgotten. However, the suggestion (Armen et al., 2004a, 2004b) that the prefibrillar form of amyloid adopts the α sheet conformation has rekindled interest in it.

Enantiomeric Polypeptides in Native Proteins

A structure (Doyle et al., 1998; Zhou et al., 2001; Watson and Milner-White, 2002b) where individual stretches of polypeptide have the alternating α_R,α_L conformation is the potassium ion specificity filter, in which four short symmetrically arranged stretches of polypeptide form the channel lining, with their main chain carbonyl oxygens pointing inwards and each coordinating directly to the column of single potassium ions being transported along it. Figure 1G shows how two peptides with this conformation form two rows of carbonyl oxygens on opposite sides of the channel that bind potassium ions. The same alternating α_R,α_L conformation is seen at one side of the water channel, also called the specificity filter, of aquaporin (Sui et al., 2001).

The right- and left-handed forms of the α conformation are close to those of the γ conformations (γ_R: $\phi = -90^\circ$, $\psi = 0^\circ$; γ_L: $\phi = 90^\circ$, $\psi = 0^\circ$) seen in Figure 2B. Although α_R,α_L alternating conformations are uncommon, γ_R,γ_L ones are abundant (Watson and Milner-White, 2002a; Pal et al., 2002; Milner-White et al., 2004) in the Protein Data Bank. An example is seen in Figure 1C. Figure 1B shows the conformation in between. The γ_R,γ_L conformations occur in stretches of two to five residues, and their main chain NH groups form a concavity with a tendency to bind single atoms, or groups of atoms, with a whole or partial negative charge, as in Figure 1F. Such features are called nests; 5%–8% of all residues in proteins are part of one. The commonest nests are those with two residues (and three nest NH groups, see Figure 1F) that occur within small hydrogen-bonded motifs. Two-residue nests exist in two enantiomeric categories, $\gamma_R\gamma_L$ (γ_R followed by γ_L), called RL, and $\gamma_L\gamma_R$, called LR. About 80% of nests are of the RL type, and 20% are LR. Wider nests, with over two residues, often bind anionic groups of atoms. In proteins that act on GTP or ATP via a P loop, the P loop includes an $\alpha_L\alpha_R\alpha_L\alpha_R$ nest, shown in Figure 5A, surrounding the β phosphate of the nucleotide.

We have described the α and γ conformations as if they are separate. However, some authors do not distinguish between α and γ, considering both to be α. Here, bold type $\boldsymbol{\alpha_R}$ or $\boldsymbol{\alpha_L}$ refers to (α_R and γ_R) or (α_L and γ_L). For present purposes, we have also allowed $\boldsymbol{\alpha_L}$ to include conformations with ψ values of up to 150°, as discussed in the Results section. Nests are defined as having two or more successive residues in the $\boldsymbol{\alpha_R,\alpha_L}$ regions. There is no obvious division between the α sheet and nest conformations, and α sheet qualifies as being composed of nests.

Amyloid and Its Prefibrillar Intermediate

From native proteins, we switch to denatured protein. The amyloid diseases are so called because they are associated with, and thought to be caused by, amyloid formation by certain proteins (Dobson, 1999; Caughey and

*Correspondence: j.milner-white@bio.gla.ac.uk

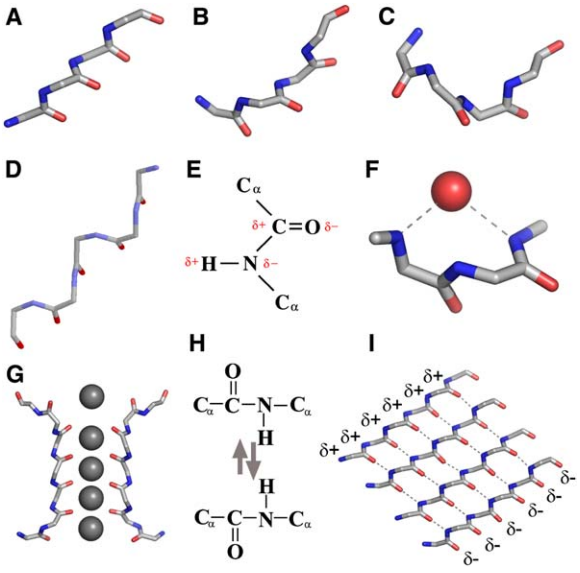

Figure 1. Conformations for Main Chain Polypeptides with Successive Enantiomeric ϕ,ψ Angles

Side chains and hydrogen atoms are omitted. (A)–(D) and (I) are models. (A) shows the α sheet conformation (ϕ = −60°, ψ = −60°; ϕ = 60°, ψ = 60°). (C) shows the nest conformation (ϕ = −90°, ψ = 0°; ϕ = 90°, ψ = 0°). (B) shows the conformation geometrically in between (ϕ = −75°, ψ = −30°; ϕ = 75°, ψ = 30°). (D) shows (A) rotated so that its characteristic S-shaped or wiggly main chain structure is apparent. (E) shows the partial charges on a -CO-NH- group. (F) shows a nest bound to a carbonyl oxygen atom; two of the NH groups are hydrogen bonded to it; typically the middle NH points slightly away. (G) shows how two peptides like that in (A) and (D) bind K^+ ions in the potassium channel (1k4c) (Zhou et al., 2001); the other two peptides forming the channel are not shown. (H) shows a diagram of a 180° peptide plane flip. (I) shows four hydrogen-bonded strands of α sheet. The arrangement of partial charges (carbonyl oxygen atoms along one edge, and NH hydrogens along the other) is characteristic. Each strand has the same conformation as (A), (D), and the middle four residues of the polypeptides in (G).

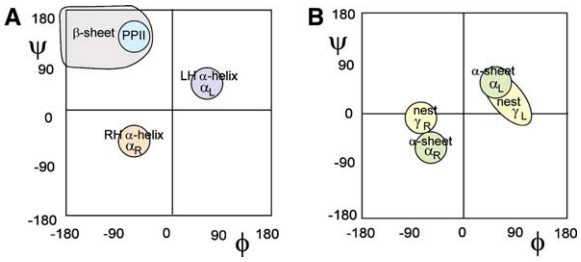

Figure 2. Ramachandran Plots Showing the ϕ,ψ Angles of Protein Features

ϕ is the torsion angle C-N-Cα-C, whereas ψ is that for N-Cα-C-N. Both are from the same amino acid residue. The α_R, α_L, γ_R, γ_L conformation terminology is indicated. In the text, bold type $\boldsymbol{\alpha_R}$ refers to the combination of α_R and γ_R; bold type $\boldsymbol{\alpha_L}$ refers to α_L plus γ_L. (A) shows the commonest structures in native proteins where the ϕ,ψ angles of successive residues are identical: α helices, β sheet, and polyproline type II helices (PPII). (B) shows structures where the ϕ,ψ angles of adjacent residues are enantiomeric; for each structure, the two pairs of values are indicated. Typical conformations for nests (Figure 1F) and α sheet (Figure 1I) (its conformation resembles that of the potassium channel selectivity filter in Figure 1G) are shown.

Lansbury, 2003). They are prevalent in old age and include Alzheimer's disease, Parkinson's disease, type II diabetes, prion diseases like BSE, and several less well-known conditions. Amyloid is found in a wide range of organisms (Chernoff, 2004). It is an insoluble, fibrillar aggregate of protein visible in the electron microscope. Biophysical studies of amyloid indicate a characteristic regularly repeating structure at the atomic level that is the same for all proteins. A number of structures have been proposed for amyloid, but various stacked parallel or antiparallel β sheet arrangements, including the β helix, are most popular (Jaroniec et al., 2002; Tycko, 2000; Peltkova et al., 2002; Klimov and Thirumalai, 2004; Makin et al., 2005; Nelson et al., 2005).

The most damaging and aggressive aspect of most amyloid proteins toward cells is not the insoluble amyloid itself but rather a soluble oligomeric prefibrillar intermediate (Caughey and Lansbury, 2003; Kayed et al., 2003; Buccianti et al., 2002; Shorter and Lindquist, 2004), which is globular in shape and much smaller than the mature amyloid fibers. It can be observed as an intermediate in amyloid formation and can also be detected in vivo. Its atomic structure is uncertain but is under active investigation. Various forms of β sheet structure or polyproline type II helix (Blanch et al., 2000) have been suggested. Since it has been shown (Fandrich et al., 2001) that most proteins form amyloid given appropriate environments, it is thought the conformations of both amyloid and its intermediate are ones all proteins have the potential to adopt. Antibodies against the prefibrillar intermediate have been raised (Kayed et al., 2003; Glabe, 2004) that recognize a conformational aspect of it. These antibodies can bind to all such intermediates, irrespective of protein type or the amino acid sequence. They also inhibit its toxicity. They do not bind to the monomeric proteins or to mature amyloid fibers. All this points to a main chain conformational feature, rather than one involving side chains, that is only present in the prefibrillar intermediate.

Conformational Changes in Amyloid Formation?

Molecular dynamic simulations (Armen et al., 2004a, 2004b, 2005; Armen and Daggett, 2005) of protein fragments of known three-dimensional structure that are active in amyloid formation, indicate that the β sheet part readily metamorphoses into α sheet under mildly denaturing conditions favoring amyloid. The authors propose that α sheet is the key constituent of the prefibrillar intermediate. The work has attracted considerable attention (Surridge, 2004; Smith, 2004). Evidence from other sources such as solid-state NMR (Jaroniec et al., 2002) and hydrogen exchange measurements (Liu et al., 2000a, 2000b) is consistent with this proposal. Even so, a hypothesis based mainly on simulations might not be thought to be convincing enough to make such a claim, but, taken along with our findings on peptide plane flipping and some observations of the magnetic effects on amyloid (Malinchik et al., 1998), it does make a persuasive case.

Peptide Plane Flipping

An appreciation of peptide plane flipping (Hayward, 2001) is crucial. Peptide flips used to be a topic of interest largely for those involved in 3D structure

determination (Kleywegt, 1996) and molecular simulations. Now there is increasing realization of its importance. Conformational changes in the main chain parts of proteins are limited by their being relatively well anchored at each end, compared with side chains that can rotate freely. A type of motion that is favored is the peptide plane flip, meaning a 180° rotation of the -CO-NH- peptide plane, as in Figure 1H, with comparatively little effect on the rest of the polypeptide including the side chains. In other words, ψ of the first residue and ϕ of the second residue change, but other angles are relatively unaffected. Certain peptide plane flips are sterically particularly favorable because they require only minor adjustments in the orientation of the adjoining peptide planes: the one most commonly observed (Gunasekharan et al., 1998) allows the interconversion of type I and type II β turns. However, we are primarily concerned with α sheet. Taking a set of protein chains with 90% or more sequence identity, we have searched for examples of interconversions of flips between β sheet and the RL form of α sheet. The results reveal numerous examples and also that the α_R,α_L α sheet conformation, uncommon in proteins in general, is surprisingly frequent in this situation. On the other hand the interconversion between β sheet and the LR form of α sheet is much less common. This is as expected because previous work (Hayward, 2001) shows that such a transition does not occur readily via peptide plane flipping.

Results

The searches for $\beta\beta \leftrightarrow \alpha_R\alpha_L$ interconversions within the 5464 protein families reveal hundreds of transitions consistent with flips. The maximum density of the "α_L" conformations found is in the region of the plot well above the main region normally regarded as α_L, as seen in Figure 3A. The α_L range was therefore extended in this direction of the plot, as far as $\psi = 150°$, to ensure most flips were included. Such conformations do still correspond to flips because that ψ value does not affect the flip in question. The analysis showed that 462 families had at least one such transition. In all, 580 $\beta\beta \leftrightarrow \alpha_R\alpha_L$ transitions were identified. At least one $\beta\beta \leftrightarrow \alpha_R\alpha_L$ transition occurs within 8.5% of families, and they are therefore not uncommon.

In Figure 3A, the comparison between the average ϕ,ψ angles from the simulations of Armen et al. (2004a), shown as blue spots, with the distribution of ϕ,ψ angles from the $\beta\beta \leftrightarrow \alpha_R\alpha_L$ flips identified from the protein families reveals a general similarity. The tendency, in both cases, for the α_L conformation to be in the normally unpopulated region at around $\phi = 60°$, $\psi = 90°$ can be explained, in terms of $\beta\beta \leftrightarrow \alpha_R\alpha_L$ flips, by constraints, probably involving hydrogen bonding, on small compensatory rotations by the peptide planes adjacent to the flipping plane, minimizing the changes in the ψ and ϕ rotation angles governing these planes. This is discussed further in the next section. Bearing this in mind, the distribution of these values is as expected for 180° flips from the β region.

The number of $\beta\beta \leftrightarrow \alpha_L\alpha_R$ transitions is also of interest and was examined within the same set of protein families. 148 were found, 134 families having at least one transition. Figure 3B shows the distribution of angles

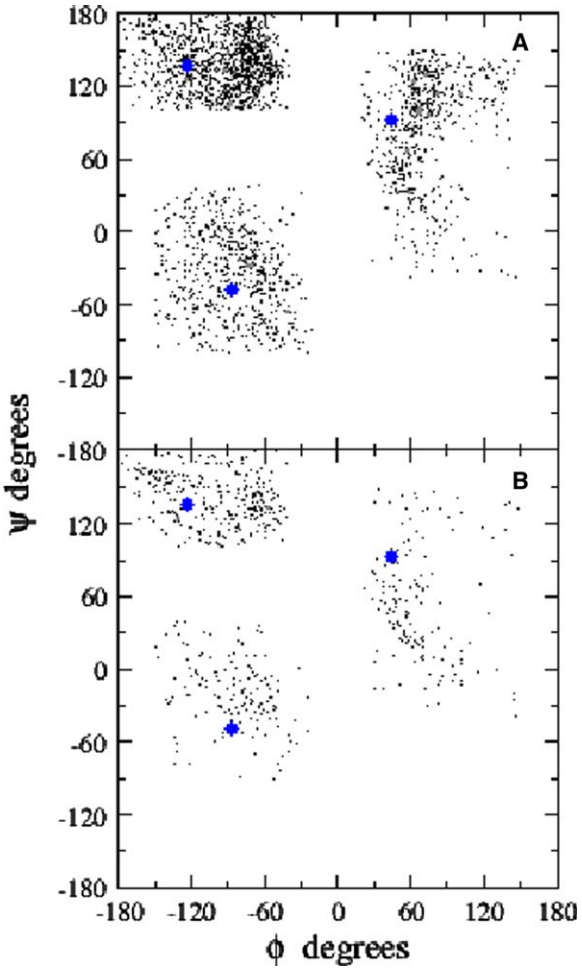

Figure 3. Distribution of ϕ,ψ Angles for the $\beta\beta \leftrightarrow \alpha_R\alpha_L$ and $\beta\beta \leftrightarrow \alpha_L\alpha_R$ Transitions

ϕ,ψ angles for the $\beta\beta \leftrightarrow \alpha_R\alpha_L$ transitions (A); ϕ,ψ angles from the $\beta\beta \leftrightarrow \alpha_L\alpha_R$ transitions (B). The average α sheet ϕ and ψ angles are from the transthyretin simulation of Armen et al. (2004b) (1tta) from the same residues in their β sheet conformation are shown by filled blue circles. It is obvious that starting from the β sheet conformation, a simple flip with no adjustment adds (or subtracts) 180° to ψ of the first residue and ϕ of the second residue. The associated adjustments, as indicated in Figure 4A, are such that residue i moves to the α_R conformation, and residue i+1 moves toward the α_L conformation.

for these interconversions. The relative abundance of $\beta\beta \leftrightarrow \alpha_R\alpha_L$, compared to $\beta\beta \leftrightarrow \alpha_L\alpha_R$, transitions is expected because the former can occur via a single flip of the intervening peptide plane, as is evident from row 21 of Table 2 of Hayward (2001). Some similarity of the distribution of ϕ,ψ angles in the $\beta\beta \leftrightarrow \alpha_L\alpha_R$, compared to $\beta\beta \leftrightarrow \alpha_R\alpha_L$, transitions may be because a number result from flipping by adjacent peptide planes. Table 2 in the present paper shows that 19 out of the 148 $\beta\beta \leftrightarrow \alpha_L\alpha_R$ transitions are next to $\beta\beta \leftrightarrow \alpha_R\alpha_L$ ones.

Table 1 gives the average ϕ and ψ values for the residues undergoing these transitions. The α_L conformation ψ values are considerably lower in the $\beta\beta \leftrightarrow \alpha_L\alpha_R$ than the $\beta\beta \leftrightarrow \alpha_R\alpha_L$ transition. The difference is statistically significant, as shown in the Experimental Procedures section. This is consistent with the frequent occurrence of

Table 1. Average ϕ,ψ Values, in Degrees, for the Transitions of Figure 3

	Residue	Mean ϕ (± SD)	Mean ψ (± SD)
$\beta_1\beta_2 \leftrightarrow \alpha_R\alpha_L$	β_1	−98 (±31)	146 (±19)
(580 examples)	β_2	−91 (±29)	137 (±20)
	α_R	−86 (±29)	−34 (±29)
	α_L	73 (±26)	86 (±26)
$\beta_1\beta_2 \leftrightarrow \alpha_L\alpha_R$	β_1	−103 (±34)	140 (±19)
(148 examples)	β_2	−96 (±33)	140 (±20)
	α_R	−84 (±29)	−21 (±29)
	α_L	69 (±29)	29 (±47)

unexpectedly high α_L values for the $\beta\beta \leftrightarrow \alpha_R\alpha_L$ transitions being due to direct peptide plane flips.

Table 2 lists details of the longer β- to α sheet flips that were found. Among the families, one $\beta\beta\beta\beta \leftrightarrow \alpha_R\alpha_L\alpha_R\alpha_L$ transition, eleven $\beta\beta\beta \leftrightarrow \alpha_R\alpha_L\alpha_R$ transitions, and seven $\beta\beta\beta \leftrightarrow \alpha_L\alpha_R\alpha_L$ transitions were found. A reason for more $\beta\beta\beta \leftrightarrow \alpha_R\alpha_L\alpha_R$ than $\beta\beta\beta \leftrightarrow \alpha_L\alpha_R\alpha_L$ is that the former requires a peptide plane flip between the first two residues, alongside a change in conformation of the third residue from β to α_R, whereas the latter peptide plane flip is accompanied by the less favored conformational change of the first residue from β to α_L.

Discussion

β- to α Sheet Conversion: Flip Geometry

In this section, the geometry of the β- to α sheet conversion is analyzed based on the average dihedral angles reported from the simulations of transthyretin (PDB code: 1tta, subunit A) by Armen et al. (2004a). The average ϕ,ψ dihedral angles are $\beta: \phi = -123^\circ, \psi = 136^\circ$; $\alpha_R: \phi = -87^\circ, \psi = -49^\circ$; $\alpha_L: \phi = 45^\circ, \psi = 92^\circ$ (from Table 2 of that paper). We show that the transition occurs by the flipping of alternate peptide planes. The conversion from β sheet to α sheet, with its alternating α_R and α_L conformations, as in Figure 4A, can be described in terms of a pair of transitions:

$$\beta(i)\beta(i+1) \rightarrow \alpha_R(i)\alpha_L(i+1) \quad (1)$$

$$\beta(i+1)\beta(i+2) \rightarrow \alpha_L(i+1)\alpha_R(i+2) \quad (2)$$

As $\Delta\phi(i+2) = \Delta\phi(i)$ and $\Delta\psi(i+2) = \Delta\psi(i)$ (see Figure 4A), there are four unique dihedral angle changes: $\Delta\psi(i), \Delta\phi(i+1), \Delta\psi(i+1)$, and $\Delta\phi$(i+2). For transition (1) above, the relative rotation, $\Delta\theta_{RL}$, of atomic groups flanking the peptide plane (including the two side chains) between residues i and i+1 can be written as (Hayward, 2001):

$$\Delta\theta_{RL} \approx \Delta\psi(i) + \Delta\phi(i+1) \quad (3)$$

Similarly, for transition (2), the relative rotation $\Delta\theta_{LR}$ of atomic groups flanking the peptide plane between residues i+1 and i+2 can be written as:

$$\Delta\theta_{LR} \approx \Delta\psi(i+1) + \Delta\phi(i+2) \quad (4)$$

Using the average dihedral angles given above, we find $\Delta\psi(i) = 175^\circ, \Delta\phi(i+1) = -192^\circ, \Delta\psi(i+1) = -44^\circ, \Delta\phi(i+2) = 36^\circ$, which give $\Delta\theta_{RL} = -17^\circ$ and $\Delta\theta_{LR} = -8^\circ$. For $\Delta\psi$(i) and $\Delta\phi$(i+1), these values are calculated assuming that the high-energy barrier along $\phi = 0^\circ$ line is not crossed (Gunasekharan et al., 1998). For the $\beta(i)\ \beta(i+1) \rightarrow \alpha_R(i)\ \alpha_L(i+1)$ transition, $|\Delta\psi(i)| + |\Delta\phi(i+1)| = 367^\circ$, whereas $|\Delta\psi(i) + \Delta\phi(i+1)| = 17^\circ$. These angles are typical of peptide plane flips (Hayward, 2001) whereby the peptide plane between residues i and i + 1 flips upside down with little effect on the orientation of the flanking regions including the side chains. Between residues i + 1 and i + 2 there is a relatively small adjustment of the peptide plane. Thus, the β sheet to α sheet conversion occurs mainly by $\beta\beta \leftrightarrow \alpha_R\alpha_L$ peptide plane flipping at alternate peptide planes, with the

Table 2. The Longest β to α Sheet Flips

Type of Transition from Conformation 1 to 2	PDB Code, Chain Identifier of Conformation 1	Residue Numbers for Conformation 1	PDB Code, Chain Identifier of Conformation 2	Residue Numbers for Conformation 2
$\beta\beta\beta\beta(1) \leftrightarrow \alpha_R\alpha_L\alpha_R\alpha_L(2)$	1LJ5, A	334–337	1DVM, A	334–337
$\beta\beta\beta(1) \leftrightarrow \alpha_R\alpha_L\alpha_R(2)$	1T7N, A	294–296	1S5O, A	273–275
$\beta\beta\beta(1) \leftrightarrow \alpha_R\alpha_L\alpha_R(2)$	1R89, A	116–118	1TFW, A	116–118
$\beta\beta\beta(1) \leftrightarrow \alpha_R\alpha_L\alpha_R(2)$	1MIQ, B	12–14	1QS8, B	12–14
$\beta\beta\beta(1) \leftrightarrow \alpha_R\alpha_L\alpha_R(2)$	1RVG, A	137–139	1RVG, C	137–139
$\beta\beta\beta(1) \leftrightarrow \alpha_R\alpha_L\alpha_R(2)$	1H3I, A	60–62	1MT6, A	60–62
$\beta\beta\beta(1) \leftrightarrow \alpha_R\alpha_L\alpha_R(2)$	1FV1, E	106–108	1SJE, B	106–108
$\beta\beta\beta(1) \leftrightarrow \alpha_R\alpha_L\alpha_R(2)$	1TGS, Z	143–145	2TGD	143–145
$\beta\beta\beta(1) \leftrightarrow \alpha_R\alpha_L\alpha_R(2)$	1UW6, R	157–159	1UX2, F	156–158
$\beta\beta\beta(1) \leftrightarrow \alpha_R\alpha_L\alpha_R(2)$	1L5Y, A	143–145	1L5Y, B	343–345
$\beta\beta\beta(1) \leftrightarrow \alpha_R\alpha_L\alpha_R(2)$	1NVJ, D	129–131	1NVI, E	129–131
$\beta\beta\beta(1) \leftrightarrow \alpha_R\alpha_L\alpha_R(2)$	1BUO, A	65–67	1CS3, A	65–67
$\beta\beta\beta(1) \leftrightarrow \alpha_L\alpha_R\alpha_L(2)$	1R1P, B	51–53	1R1S, G	51–53
$\beta\beta\beta(1) \leftrightarrow \alpha_L\alpha_R\alpha_L(2)$	1PQF, A	22–24	1PPY, B	22–24
$\beta\beta\beta(1) \leftrightarrow \alpha_L\alpha_R\alpha_L(2)$	1IAR, A	38–40	1RCB	38–40
$\beta\beta\beta(1) \leftrightarrow \alpha_L\alpha_R\alpha_L(2)$	1DCL, B	40–42	2MCG, 2	40–42
$\beta\beta\beta(1) \leftrightarrow \alpha_L\alpha_R\alpha_L(2)$	1A1M, A	43–45	1MI5, A	43–45
$\beta\beta\beta(1) \leftrightarrow \alpha_L\alpha_R\alpha_L(2)$	1D7K, B	347–349	1D7K, A	347–349
$\beta\beta\beta(1) \leftrightarrow \alpha_L\alpha_R\alpha_L(2)$	1UVM, B	2–4	1HI8, A	2–4

The majority of the 580 $\beta\beta \leftrightarrow \alpha_R\alpha_L$ and the 148 $\beta\beta \leftrightarrow \alpha_L\alpha_R$ flips found were not adjacent to each other, but a few were. They give rise to longer α- to β sheet flips, which are listed.

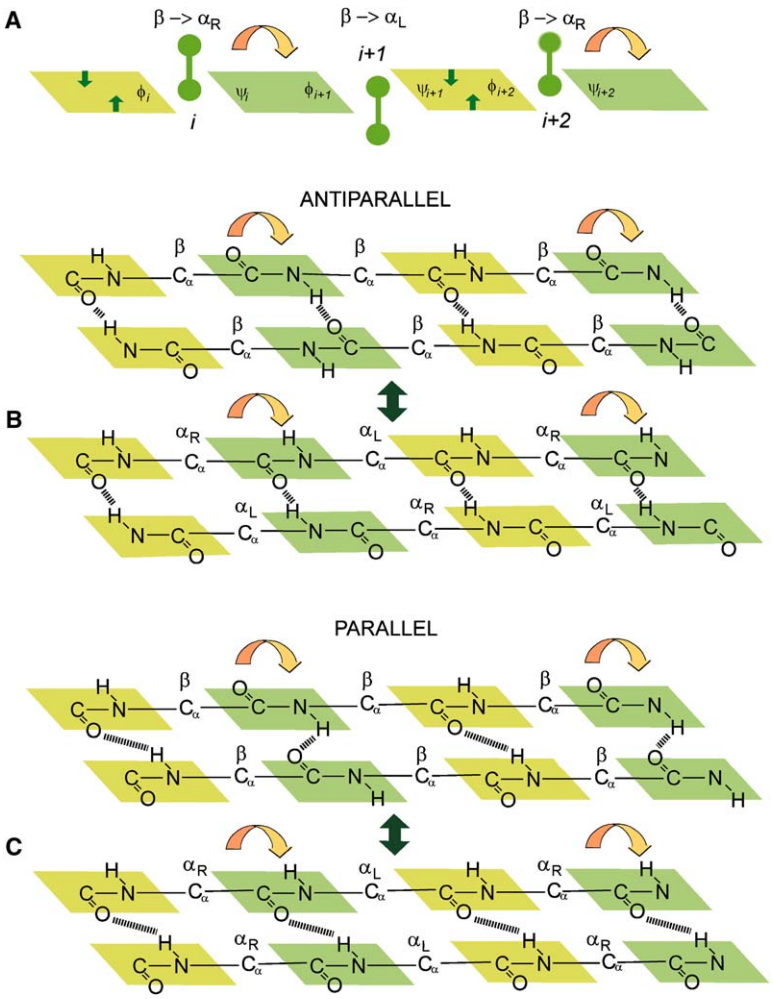

Figure 4. β Sheet to α Sheet Transition

(A) Starting from a β strand, alternating peptide planes flip roughly 180° to form $\alpha_R\alpha_L$ planes within an α strand. The intervening $\alpha_L\alpha_R$ peptide planes undergo an adjustment of about 36° in the opposite direction. C_α atoms and side chains are indicated as connected spheres.

(B and C) shows the main chain hydrogen bond arrangements for two strands of antiparallel β sheet before (above) and after (below) it flips to form α sheet; (C) shows the hydrogen bonding for a two-stranded parallel β- to α sheet interconversion. The peptide planes that undergo a 180° flip during these transitions are shaded darker green. In both (B) and (C), half of the hydrogen bonds, those connecting the pale green peptide planes, are retained.

minor $\beta\beta \leftrightarrow \alpha_L\alpha_R$ rearrangement occurring naturally as a consequence.

The unusual α_L ϕ,ψ angles observed in some of the $\beta\beta \leftrightarrow \alpha_R\alpha_L$ families can be explained by the adjacent nonflipping plane being hydrogen bonded. A $\beta(i)\ \beta(i+1) \leftrightarrow \alpha_R(i)\alpha_L(i+1)$ flip involves large changes in $\psi(i)$ and $\phi(i+1)$, which govern the flipping plane between residues i and i + 1. The $\psi(i + 1)$ and $\phi(i + 2)$ angles, which control the nonflipping plane, change by a much smaller, but significant, amount. Thus, if the rotation of this plane is constrained by hydrogen bonds when the preceding plane flips, the changes in $\psi(i + 1)$ and $\phi(i + 2)$ are hindered, as observed.

Flipping Is Favored at RL, Not LR, Nests

Analysis of the principles underlying peptide plane flipping to and from nests reveals a difference between RL and LR nests, including the corresponding α sheet conformations. It has already been pointed out that RL nests can easily flip to β sheet. Because LR nests are main chain enantiomers, they might be supposed to equally readily flip to the enantiomeric form of the β sheet conformation. These two types of flip are listed in rows 21 and 12 of Table 2 of Hayward (2001). However, the enantiomeric β conformation is rare in proteins made from L-amino acids because of steric hindrance by the side chain, so such flips are also rare. It seems likely this provides a reason for the previously unexplained phenomenon (Pal et al., 2002) that RL nests are more commonly seen than LR nests. It also explains why the peptide planes that flip by 180° within β sheet are those that give rise to the RL, not the LR, peptide planes.

Further support for this idea comes from the numbers of the two types of flips, or transitions, observed in our results. The ratio of $\beta\beta \leftrightarrow \alpha_R\alpha_L$, compared to $\beta\beta \leftrightarrow \alpha_L\alpha_R$, transitions is 3.9. This is remarkably similar to the ratio, 4.0, of RL to LR nests that are found (Watson and Milner-White, 2002b; Pal et al., 2002).

One example of $\beta\beta \leftrightarrow \alpha_R\alpha_L$ peptide plane flipping is seen in the P loop proteins (Ramakrishnan et al., 2002). These are the commonest group of proteins that catalyze phosphoryl transfer from ATP or GTP. The P loop itself incorporates an $\alpha_L\alpha_R\alpha_L\alpha_R$ nest (Watson and Milner-White, 2002b), shown in Figure 5A, with its NH groups surrounding the β-phosphate of the nucleotide's β-phosphate. In Figure 5B, the nucleotide is not bound, with the effect that the NH groups are no longer bound to an anion, giving rise to a single $\alpha_R\alpha_L \leftrightarrow \beta\beta$ flip, which is clearly visible.

Aspects of α- to β Sheet Interconversion

Considering peptide plane flipping of nests, if a strand of β sheet changes into an α sheet strand by this process, only alternate peptide planes flip, the ones that give rise

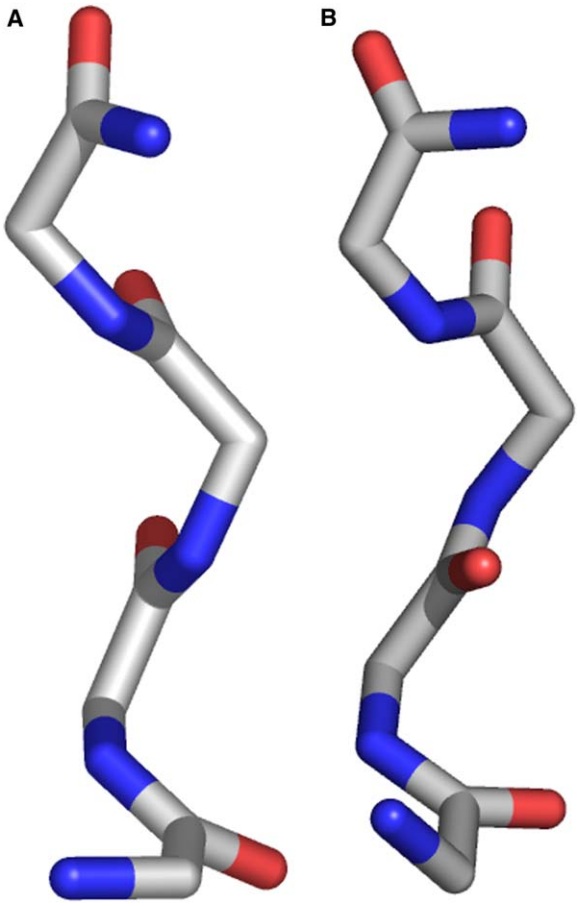

Figure 5. An Example of $\alpha_R\alpha_L \leftrightarrow \beta\beta$ Peptide Plane Flipping

The main chain atoms of residues 42–46 (for residue 46, only the nitrogen atom is shown) of the P loop of UvrB-DNA helicase are shown. (A) shows the LRLR nest from the nucleotide phosphate bound protein (PDB code 1d9z) (Theis et al., 1999); the ligand phosphate binds to the nest but is not shown. (B) shows the ligand-free enzyme (1d9x) in which the central CONH group has flipped by 180°.

to the RL peptide planes. The hydrogen bonds between the nonflipping planes are retained, becoming the LR peptide planes. Both α sheet and β sheet have the same number of hydrogen bonds. Also, in a multistrand sheet, rows of peptide planes would be expected to flip simultaneously, like dominoes. This is illustrated in Figure 4. Comparing blocks, or multiple layers, of α sheet and β sheet in three dimensions, there are striking similarities. Because the side chains do not alter much in position during peptide plane flipping, the alternation between main chain atom layers and side chain atom layers remains, with side chains from successive residues lying above and below the sheet. Furthermore the S shapes or wiggles of the main chain of α sheet strands, as in Figure 1D, correspond to the zigzag of the pleat of the β sheet.

In folded proteins from the Protein Data Bank, β sheets often exhibit considerable twist. However, the large blocks of stacked β sheet expected in amyloid cannot have much twist. It is intriguing that FTIR spectroscopy (Zandomeneghi et al., 2004), X-ray crystallography (Nelson et al., 2005), and NMR studies (Ritter et al., 2005) all indicate a lower degree of twist, as well as a more regular structure, in mature amyloid fibrils compared to that in folded proteins. This is relevant to α sheet because it is also expected to have low twist, so should interconvert more readily with the β sheet in amyloid fibrils than with that in folded proteins. Furthermore, the twisted β sheet found in folded proteins is inherently limited in size because it splays at the ends of strands. It is possible that forming β sheets via α sheet intermediates might be a good way to make large 3D blocks of β sheet.

Significant diamagnetic anisotropy is found (Malinchik et al., 1998) for the assembly of the oriented amyloid fibers. It is manifest by a magnetic field causing the growing fibers to orient in a regular way, such that X-ray fiber diffraction studies are effective. As for α-helical fibers, for which a similar magnetic effect is observed (Worchester, 1978), this can be explained by all the -CO-NH- dipoles pointing in the same direction. By contrast, in β sheet, where the magnetic effect is less marked, adjacent dipoles lie antiparallel to each other so they tend to cancel out. These dipoles derive from the partial charges (Milner-White, 1997) of the -CO-NH- atoms, as in Figure 1E. In nests, the dipoles are employed to bind anionic, or partially anionic, atoms, as in Figure 1F, whereas in α sheet, they are used to bind successive strands of sheet together, as in Figure 1H; this may account for the aggressive nature of self-assembly of amyloid. These interactions can also be described in terms of hydrogen bonding, but it is useful to consider their electrostatic nature too.

Although direct evidence for the α sheet being the key structure of the toxic intermediate is currently lacking, it provides a distinctive main chain feature that would be easily recognizable by antibodies and is likely to interconvert with β sheet. Furthermore its tendency to self-assemble into polarized sheets that would naturally attract further peptides provides an explanation for the otherwise mystifying toxicity of a polypeptide main chain conformation.

Two Polypeptide Categories: Regularly Repeating and Enantiomeric

Returning to polypeptide conformations in general, one way to visualize the range of possible structures that occur is to plot the two variable ones, ϕ and ψ, against each other. In the Ramachandran plot in Figure 2A, the positions of the conformations that have identical main chain conformations for successive residues, α helix, β sheet, and PPII helix, are added. Figure 2B gives the same Ramachandran plot with the positions of the enantiomeric nest and α sheet conformations marked. Pairs of ϕ,ψ values are from individual amino acids and successive enantiomeric residues are related by multiplying their ϕ and ψ values by −1, so each type of conformation appears twice on the plot in symmetrical positions.

The nest conformation is the one most commonly found in proteins, yet the α sheet conformation is found comparatively rarely and only in single polypeptides. This might seem surprising as the α sheet is expected to be energetically comparatively favorable. However, being so dangerous, amyloidogenic structures, unless buried in some way, are expected to have been eliminated during evolution, as has been suggested (Dobson, 1999), which would explain the infrequency of the α sheet conformation in native proteins.

Conclusion

Evidence supporting the idea (Armen et al., 2004a) that α sheet is the key toxic component of the soluble prefibrillar form of amyloid is presented. It is proposed that amyloid formation occurs in two stages. The first is the assembly of unfolded polypeptides to form α sheet; the second is the transformation, by means of peptide plane flipping, of α sheet into β sheet, the mature form of amyloid. The α sheet conformation can be regarded as a flattened version of the nest (Watson and Milner-White, 2002a), an anion binding feature in proteins. Both belong to a category of polypeptides where the main chain parts of successive amino acid residues are enantiomeric (Watson and Milner-White, 2002b). While 5%–8% of amino acid residues in soluble proteins form nests, the α sheet conformation is strangely rare, considering the steric accessibilities of the component amino acids in that state; this may result from its toxicity, causing proteins with it to be eliminated during evolution. Two short stretches of polypeptide that adopt the α sheet conformation are the selectivity filters of the potassium channel (Zhou et al., 2001) and aquaporin (Sui et al., 2001).

Our analysis of protein conformations of very closely related families of protein crystal structures show that dipeptide interconversions of the type $\beta\beta \leftrightarrow \alpha_R\alpha_L$ occur commonly. 580 examples were found; 8.5% of protein families exhibit at least one such transition. Dipeptide interconversions of the type $\beta\beta \leftrightarrow \alpha_L\alpha_R$ were also counted and about 25% of the number were found. This is in accord with work (Hayward, 2001) on peptide plane flipping that identifies $\beta\beta \leftrightarrow \alpha_R\alpha_L$ as geometrically likely to occur via isolated peptide plane flips, whereas $\beta\beta \leftrightarrow \alpha_L\alpha_R$ is difficult because it gives rise to much more disturbance to adjacent parts of the polypeptide chain. During this survey, the range of ψ angles for the α_L residue was extended beyond the usual range to 150° because its value does not affect the degree of flip. Such "α_L" values, although in a less favored region of the Ramachandran plot, are as expected for direct flips, and especially where the flanking peptide planes, being hydrogen bonded, are restricted in their movements when the flip occurs. Overall, these observations show that RL nests, including short strands of α sheet and related structures, often interconvert with β strands via peptide plane flips.

This leads to two conclusions. One relates to nests in general: it appears that RL nests are more commonly found in folded proteins than LR nests because β sheet peptides readily flip to form RL, but not LR, nests. The other is that $\alpha_R\alpha_L \leftrightarrow \beta\beta$ flips of alternate peptide planes along a strand facilitate the α sheet to β sheet interconversion process proposed to generate mature amyloid. This is illustrated in Figure 4. In three dimensions, mature amyloid is thought to consist of layers of flat untwisted β sheet. A similar structure is envisaged for α sheet in the prefibrillar intermediate. The arrangement of main chains and side chains in the two types of sheet is strikingly similar. Thus, the major change involved in the interconversion of layers of α and β sheet is the concerted peptide flipping of peptide planes, while any concomitant side chain adjustments are relatively minor. These considerations indicate that the α sheet to β sheet interconversion is far less implausible than it might appear at first sight.

Experimental Procedures

To search for flips between closely related proteins, a method used previously (Qi et al., 2005), and summarized below, was employed to generate "families." NMR structures, theoretical models, nonprotein structures, and proteins of less than 40 amino acids were removed from the July 2005 release of the Protein Data Bank (PDB). Chains with more than 10% of their residues labeled "unknown" were also removed, resulting in 60,629 sequences. Removing structures solved to a resolution greater than 2.5 Å resulted in 41,375 sequences. The longest sequence was aligned pairwise with every other sequence in the list. Proteins having sequences with 90% or greater sequence identity with it were assigned as a "family," the longest being the "family representative." This family was removed from the list. The longest sequence in the new list was chosen as the next representative and the process repeated till exhaustion. The algorithm is similar to that of the program CD-HIT (Li et al., 2001). The process resulted in 5464 families, each containing 2 or more members, 1 of which is the representative member.

To search for $\beta\beta \leftrightarrow \alpha_R\alpha_L$ and $\beta\beta \leftrightarrow \alpha_L\alpha_R$ transitions, the following procedure was carried out on every family. Each residue in a family of proteins was assigned to be in the β region if $-180° < \phi < -40°$ and $100° < \psi < 180°$, the α_R region if $-150° < \phi < -20°$ and $-100° < \psi < 40°$, and the α_L region if $20° < \phi < 150°$ and $-40° < \psi < 150°$. If adjacent residues were $\beta\beta$ in a family member and the corresponding residues (according to the sequence alignment) were $\alpha_R\alpha_L$ in the representative member, or vice-versa, a $\beta\beta \leftrightarrow \alpha_R\alpha_L$ transition was recorded. The $\beta\beta \leftrightarrow \alpha_L\alpha_R$ transitions were recorded similarly. This was carried out between all family members and the representative. To avoid over counting if the representative is in one conformation and more than one family member is in another, only one transition per pair of sequentially adjacent residues per family was counted.

To determine if the differences in the mean ψ values for the two sets of α_L conformations in Figure 3 are statistically significant, a two-sample t test was employed by using $t = \left(\psi_2 - \psi_1\right)\sqrt{(\sigma_1^2/N_1 + \sigma_2^2/N_2)}$ where ψ_2, N_2, and σ_2 are the mean ψ value, the number of examples, and the standard deviation for the $\beta\beta \leftrightarrow \alpha_R\alpha_L$ transition and ψ_1, N_1, and σ_1 are the mean ψ value, the number of examples, and the standard deviation for the $\beta\beta \leftrightarrow \alpha_L\alpha_R$ transition. Using the data in Table 1 gives t = 7.2, which is highly significant.

Received: May 31, 2006
Revised: June 28, 2006
Accepted: June 28, 2006
Published: September 12, 2006

References

Armen, R.S., and Daggett, V. (2005). Characterization of two distinct β_2-microglobulin unfolding intermediates that may lead to amyloid fibres of different morphology. Biochemistry *44*, 16098–16107.

Armen, R.S., DeMarco, M.L., Alonso, D.O.V., and Daggett, V. (2004a). Pauling and Corey's α-pleated sheet structure may define the prefibrillar amyloidogenic intermediate in amyloid disease. Proc. Natl. Acad. Sci. USA *101*, 11622–11627.

Armen, R.S., Alonso, D.O.V., and Daggett, V. (2004b). Anatomy of an amyloidogenic intermediate: conversion of β-sheet to α-sheet structure in transthyretin at acid pH. Structure *12*, 1847–1863.

Armen, R.S., Bernard, B.M., Day, R., Alonso, D.O.V., and Daggett, V. (2005). Characterization of a possible amyloidogenic precursor in glutamine-repeat neurodegenerative diseases. Proc. Natl. Acad. Sci. USA *102*, 13433–13438.

Blanch, W., Morozova-Roche, L.A., Cochran, D.A.E., Doig, A.J., Hecht, L., and Barron, L.D. (2000). Is polyproline II helix the killer conformation? A Raman optical activity study of the amyloidogenic prefibrillar intermediate of human lysozyme. J. Mol. Biol. *301*, 553–563.

Buccianti, M., Giannoni, E., Chiti, F., Barone, F., Formigli, L., Zurdo, J., Taddei, N., Ramponi, G., Dobson, C.M., and Stefani, M. (2002). Inherent toxicity of aggregates implies a common mechanism for protein folding diseases. Nature *416*, 507–511.

Caughey, B., and Lansbury, P.T. (2003). Protofibrils, pores, fibrils and neurodegeneration: separating responsible protein aggregates from innnocent bystanders. Annu. Rev. Neurosci. *26*, 267–298.

Chernoff, Y.O. (2004). Amyloidogenic domains, prions and structural inheritance: rudiments of early life or recent acquisition? Curr. Opin. Chem. Biol. *8*, 665–671.

Dobson, C.M. (1999). Protein misfolding, evolution and disease. Trends Biochem. Sci. *24*, 329–332.

Doyle, D.A., Cabral, J.M., Pfuezner, R.A., Kuo, A., Gulbis, J.M., Cohen, S.L., Chait, B.T., and Mackinnon, R.T. (1998). The structure of the potassium channel: molecular basis of K+ conduction and selectivity. Science *280*, 69–77.

Fandrich, M., Fletcher, M.A., and Dobson, C.M. (2001). Amyloid fibrils from muscle myoglobin. Nature *410*, 165–166.

Glabe, C.G. (2004). Conformation-dependent antibodies target diseases of protein misfolding. Trends Biochem. Sci. *29*, 542–547.

Gunasekharan, K., Gomathi, L., Ramakrishnan, C., Chandrasekhar, J., and Balaram, P. (1998). Conformational interconversions in peptide β-turns: analysis of turns in proteins and computational estimates of barriers. J. Mol. Biol. *284*, 1505–1516.

Hayward, S. (2001). Peptide plane flipping in proteins. Protein Sci. *10*, 2219–2227.

Jaroniec, C.P., MacPhee, C.E., Astrof, N.S., Dobson, C.M., and Griffin, R.G. (2002). Molecular conformation of a peptide fragment of transthyretin in an amyloid fibril. Proc. Natl. Acad. Sci. USA *99*, 16748–16753.

Kayed, R., Head, E., Thompson, J.L., McIntyre, T.M., Milton, S.K., Cotman, C.W., and Glabe, C.G. (2003). Common structure of soluble amyloid oligomers implies a common mechanism of pathogenesis. Science *300*, 486–489.

Kleywegt, G. (1996). Use of non-crystallographic symmetry in protein refinement structure. Acta Crystallogr. D Biol. Crystallogr. *52*, 842–857.

Klimov, D.K., and Thirumalai, D. (2004). Dissecting the assembly of Aβ(16–22) amyloid peptides into antiparallel β-sheets. Structure *11*, 295–307.

Li, W., Jaroszewski, L., and Godzik, A. (2001). Clustering of highly homologous sequences to reduce the size of large protein databases. Bioinformatics *17*, 282–283.

Liu, K., Cho, H.S., Hoyt, D.W., Nguyen, T.N., Olds, P., Kelly, J.W., and Wemmer, D.E. (2000a). Deuterium-proteon exchange on the native wild-type transthyretin tetramer identifies the stable core of the individual subunits and indicates motility at the subunit interface. J. Mol. Biol. *303*, 555–565.

Liu, K., Cho, H.S., Laushuel, H.A., Kelly, J.W., and Wemmer, D.E. (2000b). A glimpse of a possible amyloidogenic intermediate of transthyretin. Nat. Struct. Biol. *7*, 754–757.

Makin, O.S., Atkins, E., Sikorski, P., Johansson, J., and Serpell, L.C. (2005). Molecular basis for amyloid fibril formation and stability. Proc. Natl. Acad. Sci. USA *102*, 315–320.

Malinchik, S.B., Inouye, H., Szumowski, K.E., and Kirschner, D.A. (1998). Structural analysis of Alzheimer's β(1–40) amyloid: proteofilament asembly of tubular fibrils. Biophys. J. *74*, 537–545.

Milner-White, E.J. (1997). The partial change of the nitrogen atom in peptide bonds. Protein Sci. *6*, 2477–2482.

Milner-White, E.J., Nissink, J.W.M., Allen, F.H., and Duddy, W.J. (2004). Recurring main chain anion-binding motifs in short polypeptides. Acta Crystallogr. D Biol. Crystallogr. *60*, 1935–1942.

Nelson, R., Sawaya, M.R., Balbirnie, M., Madsen, A.O., Riekel, C., Grothe, R., and Eisenberg, D. (2005). Structure of the cross-β spine of amyloid-like fibrils. Nature *435*, 773–778.

Pal, D., Suehnel, J., and Weiss, M. (2002). New principles of protein structure: nests, eggs and what next? Angew. Chem. *41*, 4663–4665.

Pauling, L., and Corey, R.B. (1951a). The pleated sheet, a new layer configuration of polypeptide chains. Proc. Natl. Acad. Sci. USA *37*, 251–256.

Pauling, L., and Corey, R.B. (1951b). Configurations of polypeptide chains with favored orientations around single bonds: two new pleated sheets. Proc. Natl. Acad. Sci. USA *37*, 729–740.

Peltkova, A.T., Ishii, Y., Balbach, J.J., Antzukin, O.N., Leapman, R., Deglaglio, F., and Tycko, R. (2002). A structural model for Alzheimer's β-amyloid fibrils based on experimental constraints from solid state NMR. Proc. Natl. Acad. Sci. USA *99*, 16742–16747.

Qi, G., Lee, R., and Hayward, S. (2005). A comprehensive and non-redundant database of protein domain movements. Bioinformatics *21*, 2832–2838.

Ramakrishnan, C., Dani, V.S., and Ramasarma, T. (2002). A conformational analysis of Walker motif A [GXXXXGKT(S)] in nucleotide-binding and other proteins. Protein Eng. *15*, 783–798.

Ritter, C., Maddelin, M.-L., Siemer, A.B., Luhrs, T., Ernst, M., Meier, B., Saupe, S.J., and Riek, R. (2005). Correlation of structural elements and infectivity of the HET-s prion. Nature *435*, 844–848.

Shorter, J., and Lindquist, S. (2004). Hsp 104 catalyses formation and elimination of self-replicating sup35 conformers. Science *304*, 1793–1797.

Smith, O.M. (2004). A neatly pleated sheet. Science *305*, 1534.

Sui, H., Han, B.-G., Lee, J.K., Wallan, P., and Jap, B.K. (2001). Structural basis of water-specific transport through the AQP1 water channel. Nature *414*, 872–878.

Surridge, C. (2004). New role for Pauling's ribbons. Nature *430*, 739.

Theis, K., Chen, P.J., Skorvaga, M., van Houten, B., and Kisker, C. (1999). Crystal structure of UvrB, a DNA helicase adapted to nucleotide excision repair. EMBO J. *18*, 6899–6907.

Tycko, R. (2000). Solid state NMR as a probe of amyloid fibril architecture. Curr. Opin. Struct. Biol. *4*, 500–506.

Watson, J.D., and Milner-White, E.J. (2002a). A novel main chain anion binding site in proteins: the nest. A particular combination of ϕ,ψ angles in successive residues gives rise to anion binding sites that occur commonly and are found often in functionally important regions. J. Mol. Biol. *315*, 171–182.

Watson, J.D., and Milner-White, E.J. (2002b). The conformations of polypeptide chains where the main chain parts of successive residues are enantiomeric. Their occurrence in cation and anion binding regions in proteins. J. Mol. Biol. *315*, 183–191.

Worchester, D.L. (1978). Structural origins of diamagnetic anisotropy in proteins. Proc. Natl. Acad. Sci. USA *75*, 5475–5477.

Zandomeneghi, G., Krebs, M.R.H., McCammon, M.G., and Fandrich, M. (2004). FTIR reveals structural differences between native β-sheet proteins and amyloid fibrils. Protein Sci. *13*, 3314–3321.

Zhou, Y., Morais-Cabral, J.H., and MacKinnon, R. (2001). Chemistry of ion coordination and hydration revealed by the K^+ channel-Fab complex. Nature *414*, 43–48.